Optics Letters

Ultrashort pulse Kagome hollow-core photonic crystal fiber delivery for nonlinear optical imaging

Marco Andreana, Tuan Le, Wolfgang Drexler, and Angelika Unterhuber*

Center for Medical Physics and Biomedical Engineering, Medical University of Vienna, Waehringer Guertel 18-20/E4.L, 1090 Vienna, Austria
**Corresponding author: angelika.unterhuber@meduniwien.ac.at*

Received 17 December 2018; revised 20 February 2019; accepted 21 February 2019; posted 21 February 2019 (Doc. ID 355219); published 20 March 2019

We report ultrashort pulse delivery through a hypocycloid-core inhibited-coupling Kagome hollow-core photonic crystal fiber (HC-PCF). Undistorted 10 fs and 6.6 nJ pulses were launched through 1 m long fiber without fiber dispersion pre-compensation and 80% efficiency. The performance of this technology for biomedical imaging is demonstrated on a biological sample by incorporating the fiber into a two-photon excited fluorescence (TPEF) laser scanning microscope (LSM) achieving a pulse width of 15 fs at the sample location. To the best of our knowledge, this is the first report on undistorted TPEF imaging in a LSM with 15 fs pulses delivered through a 1 m long Kagome HC-PCF with high throughput.

https://doi.org/10.1364/OL.44.001588

Nonlinear optical imaging (NLOI) has become a powerful modality in the biomedical field for high-resolution *in vivo* imaging of physiologic and molecular distribution in biological tissue by virtue of its subcellular resolution and biochemical specificity [1]. Two-photon excited fluorescence (TPEF) providing signals either from endogenous (nicotinamide adenine dinucleotide, elastin, and flavins) or exogenous fluorophores is the most powerful variant [2]. Ultrafast lasers, in combination with high numerical aperture (NA) objectives, enable tight confinement in space and time and, thus, enhance the two-photon excitation probability due to the quadratic increase in signal intensity with respect to the excitation laser power. The result is intrinsic localized excitation with inherent three-dimensional sectioning. Ti:sapphire lasers providing high powers and single-digit femtosecond pulse durations have proven to be versatile light sources for NLOI in the near-infrared regime (NIR). They induce high nonlinear signals with reduced scattering, photo-bleaching and photo-damage, as well as improved imaging depth.

However, there are still some key challenges, which have to be addressed for *in vivo* and *in situ* imaging when fiber delivery is required. Already when using short laser pulses (usually with pulse widths shorter than 200 fs), constraints arise from pulse broadening in optical elements, especially from high NA objective lenses and fiber delivery systems. Self-phase modulation (SPM) and other nonlinear effects broaden the spectral and temporal shape of the laser pulses and normal group-velocity dispersion (GVD) restricts an undistorted pulse propagation [3]. Proper management of chromatic material dispersion is crucial to optimize the nonlinear signals, which becomes especially important for label-free functional *in vivo* applications where high-detection sensitivities are required in order to probe endogenous fluorophores that exist only in low abundance and have small two-photon action cross sections. It has been demonstrated that an increase in pulse spectral bandwidth, from 10 to 80 nm, results in an up to eight-fold TPEF signal increase [4]. In addition, the sample penetration depth and signal-to-noise ratio can be increased by these means while reducing photo-bleaching due to lower incident average powers on the sample, but only when ultrashort pulse durations (sub-20 fs) are preserved at the same time [5,6]. Furthermore, broadband excitation probes the entire bandwidth of many investigated fluorophores (~50 to 100 nm) and allows for simultaneous selective excitation without wavelength tuning and the advantage of intrinsic co-localization. Hence, the pulse width conservation of sub-20 fs pulses has important implications for applications employing NLOI and endoscopes. In particularly, for long-term sample viability, an imaging system that requires very low average light power to minimize any kind of photo-bleaching is required. On the other hand, free-space beam guiding is prone to misalignment, drifts, and vibrations, and is often disadvantageous regarding safety regulations. Great advances in optical fibers, micro-optics, and micro-mechanics have been achieved, but innovations for an optical fiber delivery lag behind and get mainly stuck in the 100 fs regime [3,7]. Therefore, one primary key challenge for wide-spread biomedical NLOI poses the delivery and preservation of ultrashort laser pulses with high fidelity through several meters of optical fibers in the NIR suitable for a clinical environment. Many methods have been proposed over the last decade, but technical challenges for the ultrashort pulse regime and for signal collection have hindered a widespread breakthrough. Single-mode fibers (SMFs), multi-mode fibers (MMFs), and photonic crystal fibers (PCFs) have been proposed to deliver nanojoule pulses. SMFs are most widely used, since they perfectly preserve the spatial beam profile making them ideal candidates for diffraction-limited focusing [8,9]. However, conventional SMFs experience large chromatic material dispersion in the 800 nm regime, where

two-photon absorption bands of most intrinsic fluorophores are located [10,11]. Furthermore, even longer pulses with sub-200 fs pulse duration experience severe temporal and spectral broadening due to GVD, SPM, and self-steepening leading to significant reductions of nonlinear signals and sample penetration depths [12,13]. Hence, ultrashort optical pulses required for NLOI are easily affected in bulk optical fibers, resulting in reduced pulse peak powers and a weak two-photon excitation at the distal end of the fiber. This is mainly due to two-photon excited photocurrent which is reduced from quadratic intensity dependence to a linear, even at low average output powers [14]. Additionally, low NA (~0.1) and small core sizes (~3 μm) make these fibers prone to optical aberrations in imaging systems. Nonlinearities can be reduced by launching the beam through large-core fibers, thereby minimizing peak intensities over a large area. However, broadening still occurs at higher intensities and, typically, several modes are supported [11,14]. Approaches to shape the input or recompress the output pulses severely increase complexity and losses [8,15–17]. MMFs have larger NAs and core sizes, but prevent focusing to a near-diffraction-limited spot due to multiple spatial modes. Up to now, the best alternative has been to use large-mode-area PCFs that have large mode field diameters (>10 μm) and guide light at any wavelength transparent for silica in single-mode operation. The SPM effect is reduced, but accurate dispersion compensation for silica is still required limiting its applicability for NLOI.

For less than two decades, low-loss optical fiber technology has emerged that guides light in a hollow core surrounded by a two-dimensional periodic cladding. A pulse propagating in such a hollow air core experiences really low dispersion and nonlinear effects. Light can be guided in a fiber by total internal reflection; a higher refractive index of the core is required compared to the cladding. This refractive index difference can be realized by a so-called Bragg photonic bandgap fiber guidance [18–20]. These fibers are suitable for high power delivery, but support a limited bandwidth while having rather small hollow-core (HC) sizes. Usually, there is a large spatial overlap between the core and the silica core wall, limiting the coupled power level for high power applications [21]. By introducing a cladding structure that consists of fine silica webs arranged in a Kagome lattice surrounded by air, thus facilitating low spatial overlap with silica, pulses with high peak intensities are guided without relying on photonics bandgap [22]. In this type of fiber, the GVD is much lower, and the wavelength range with good transmission becomes much broader [23]. Ultrashort light pulses up to microjoule level can be delivered using an air-filled Kagome fiber [21,24]. Inhibited coupling (IC) Kagome HC PCFs are a versatile means for transporting high power ultrashort laser pulses with low losses, as well as low temporal, spectral, and modal pulse distortion due to negligible dispersion and optical overlap with the silica cladding. Due to low waveguide dispersion and nonlinearity, advanced pre-compensation schemes become obsolete [25]. Hence, the delivery of ultrashort laser pulses over long distances covering a broad spectral range with intrinsic guidance properties, high damage thresholds, and low losses over wide transmission windows with ultra-low GVD can be achieved [26].

This Letter presents an investigation of a recently developed ultra-large-core hypocycloid-core IC Kagome HC-PCF for undistorted delivery of nanojoule femtosecond pulses from a broadband Ti:sapphire laser. The use of ultrashort pulses is a practical way to improve the excited nonlinear signal, e.g., in TPEF microscopy. TPEF imaging of a fixed biological sample using 10 fs pulses from an ultrafast Ti:sapphire laser delivered via 1 m long IC Kagome HC-PCF is demonstrated with no fiber dispersion compensation via prism or grating compressor.

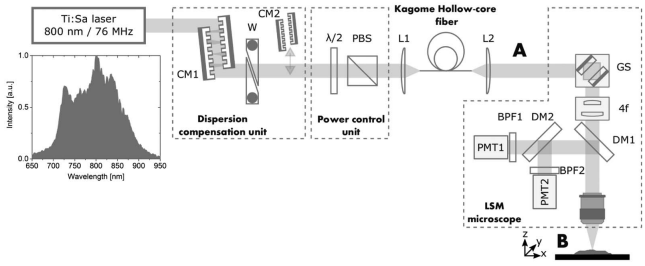

Fig. 1. Experimental setup used for characterization of the Kagome HC fiber and for imaging. CM1 and CM2, chirped mirror (CM2 is used to compensate for dispersion introduced by the LSM); W, wedges; $\lambda/2$, half-wave plate; PBS, polarization beam splitter; L1-2, lenses; GS, galvanometric scanning mirrors; $4f$, scan and tube lenses in a $4f$ telecentric configuration; DM1-2, dichroic mirror; BPF1-2, bandpass filters; PMT1-2, photomultiplier tubes. Inset, output spectrum of Ti:sapphire laser. A and B indicate the points where the laser pulse duration has been measured.

The setup, as shown in Fig. 1, is composed of a mode-locked Ti:sapphire laser oscillator, a dispersion pre-compensation unit including chirped mirrors and a pair of wedges (BK7) and the 1 m long IC Kagome HC-PCF with its coupling optics. Both chirped mirrors and wedges could be translated to change dispersion continuously between 100 fs^2 and 5000 fs^2. The compensation unit is used to obtain transform-limited pulses after re-collimation of the distal fiber output and at the focal plane of the laser scanning microscope (LSM). We compensate for the dispersion introduced by the power control unit consisting of a half-wave plate and polarization beam splitter, the coupling, and re-collimation lenses (L1, L2), as well the optics, including microscope objective in the LSM. The hypocycloid-core-contour IC Kagome HC-PCF (PMC-C-TiSa_Er-7C, GLOPhotonics, France) with optimized performance in two spectral regions (800 nm and 1600 nm) showed nearly single-mode guidance of the output of our broadband Ti:sapphire laser. The 63 μm core was surrounded by a 300 μm diameter micro structured cladding. Within its two large separated transmission windows with more than 300 nm in the 800 nm and 1600 nm wavelength regions the dispersion of this fiber was virtually constant around 1 ps/nm/km with an attenuation of less than 80 dB/km. The light travelled through 1 m long piece of this fiber with a mode field diameter of 44 μm and bending loss of 3 dB at a bending radius of less than 50 mm. The in-house built Ti:sapphire laser oscillator generated optical pulses with a bandwidth at full width at half maximum (FWHM) of ~150 nm at a repetition rate of 75 MHz and a pulse energy of 6.6 nJ. A half-wave plate in combination with a polarization beam splitter installed in front of the focusing element (L1) was used to attenuate the output power of the oscillator and to prevent the fiber facet being burned during the coupling process. The total transmission, including coupling and guiding losses was measured as 80% showing no power dependence. The near-field intensity distribution

showed a hexagonal shape pattern according to the core geometry and verified our findings that the intensity was mostly confined in the central core [27]. At the distal end of the fiber the beam was re-collimated (L2) and sent to the LSM where the diagnostic instruments, i.e. the spectrometer and autocorrelator were implemented in the focal spot of the sample. An ultrathin beam splitter was used to enable spectral and temporal characterization of the pulse from the laser (A) and at the sample plane (B) as indicated in Fig. 1. For characterization purposes the fiber was either inserted into the beam path or circumvented on the way to the custom-made upright LSM described elsewhere [28].

Higher-order modes were only observed with poor fiber coupling. Coupling between the low-loss mode and higher order modes was not seen. The autocorrelation and the spectrum of the pulses at the input and output facets were measured from 5 mW to 500 mW average output power, respectively, revealing stable quasi-fundamental mode propagation. Hence, all interferometric autocorrelation (IAC) traces were taken with power levels relevant to the sample. The IC Kagome HC-PCF showed only little material dispersion in the 800 nm regime and no nonlinear effects since the ultrashort pulses travelled through the HC, where the refractive index was uniform everywhere. The measured IAC trace of the free-space laser pulses revealed 10 fs pulse width as is shown in Fig. 2(c). The IAC after insertion of the 1 m long IC Kagome HC-PCF after the output of the Ti:sapphire laser as shown in Fig. 1 is depicted in Fig. 2(d). The pulse duration was basically preserved independently from the average transmitted power proving the preservation of the fundamental mode propagation. Only bulk optics as $\lambda/2$ half-wave plate and polarization beam splitter, coupling and re-collimation lenses as well as air had to be pre-compensated for with 5 bounces on a chirped mirror pair as part of the pre-compensation unit (~500 fs^2). Nonlinear effects were not visible in the IAC traces of Figs. 2(c) and 2(d) in the operating region up to 500 mW corresponding to pulse energies of ~6.6 nJ. Minor wings in the interferometric autocorrelation trace could be caused by small nonlinear frequency chirp due to uncompensated higher order dispersion (HOD). Assuming a $sech^2$ shape, we calculated the fiber output pulse duration to be ~10 fs. Dispersion of bulk optics of the LSM (achromatic lenses, dichroic beam splitter, microscope objective) were accounted for by adding 8 bounces on a second pair of high negative dispersive mirrors (2800 fs^2). Hence, 10 fs pulses were launched into the LSM and a ~15 fs IAC trace was measured at the focal plane of the sample as indicated in Fig. 2(b). These are to our knowledge the shortest pulses ever measured with a throughput of 80% transmitted through a 1 m long optical fiber without pre-compensation usually done with a prism or grating pre-compressor. Figure 2(b) indicates that the pulses were stretched, which is likely caused by the strong residual HOD of the microscope objective. Again, the pulse duration of 15 fs was obtained by using a $sech^2$ profile for deconvolution of the autocorrelation data. All IAC traces were optimized individually by optimizing the pre-compensation unit for the respective amount of dispersion. Figure 2(a) compares the power spectral density of the input pulse (gray area) and the output pulse (black dotted line) of the IC Kagome HC-PCF revealing that the spectral width and shape was perfectly preserved throughout the fiber which confirm that no fiber nonlinearities were involved.

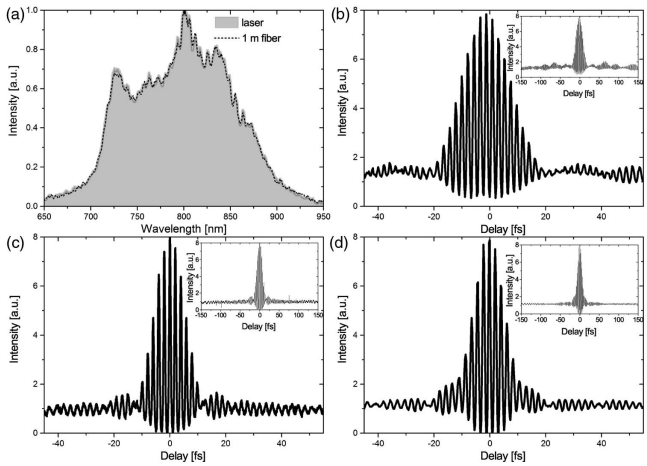

Fig. 2. (a) Measured spectra before (gray) and after propagation through 1 m of IC Kagome HC PCF (black dotted). (b) IAC indicating the pulse duration at the sample plane in the LSM (position B in Figure 1). (c) and (d) IAC traces from Ti:sapphire laser measured at position A in Fig. 1 without (c) and with inserted fiber (d).

Using 15 fs laser pulses delivered to the sample location in the LSM, the imaging capability of the tested fiber was verified on a biological sample. TPEF signals were generated from a stained tissue sample from a mouse intestine section (Molecular Probe FluoCells #4, Thermo Fischer Scientific, U.S.) labeled with a combination of two different fluorescent stains. The mucus of goblet cells and the filamentous actin prevalent in the brush border were marked with AlexaFluor350 and AlexaFluor560, respectively. The peaks of the two-photon excitation spectra of these two dyes fall within the excitation bandwidth enabling simultaneous excitation of TPEF signals [1]. The generated fluorescence signals of the dyes were collected simultaneously since the emission fluorescence spectra were well separated to each other, as well as from the excitation pulse bandwidth. Figure 3 shows the merged TPEF image where the red and green colors represent the mucus of goblet cells and the brush border of a 100 µm thick mouse intestine

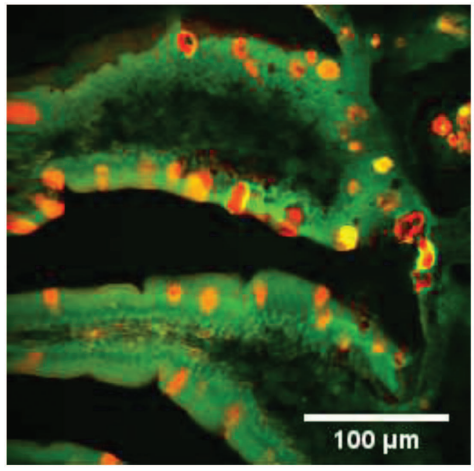

Fig. 3. Mouse intestine section: merged TPEF image (256 × 256 pixels) showing the mucus of goblet cells (AlexaFluor350, red) and the filamentous actin prevalent in the brush border (AlexaFluor560, green).

section, respectively. We simultaneously collected the generated fluorescence signals in the backward direction using a combination of bandpass filters and dichroic mirrors (ET455/50 m, ET609/34 m, T613 spxr, T560l pxr, Chroma Technology, U.S.). The image was recorded with a pixel dwell time of 6.4 μs for a field of view (FOV) of 320 μm^2, and recorded at 1.25 fps. The maximum average power used at the sample was 60 mW. With this fiber technology multiple fluorophores with well-spaced excitation spectra were excited simultaneously. The excited signal was both proportional to the overlap of the TPEF spectra of the investigated fluorophores and to the two-photon excitation spectrum achievable with the broadband laser. There is no need to tune the wavelength of the excitation laser source to match the two-photon excitation spectra peaks. Multicolor two-photon excitation is allowed since the entire laser bandwidth contributes to enhancement of the TPEF intensity with different "multicolor" combinations. This becomes a key factor in environments where the applicable optical power on the sample is limited by cell-damage or photo-bleaching.

In summary, we demonstrated a high throughput almost undistorted 10 fs pulse fiber delivery through a 1 m–long IC Kagome HC-PCF without bulk fiber pre-compensation. The Kagome HC-PCF is found to be favorable as an ultrashort pulse delivery for multicolor TPEF imaging. 15 fs laser pulses are successfully recorded at the sample plane of a LSM, whereas pulse duration was only limited by the HOD of the objective. To the best of our knowledge, this is the first report on TPEF imaging with 15 fs pulses sent through a 1 m fiber delivery. This implication has significant impact in enhancing the NLOI intensity by using optical pulses in the sub-20 fs regime. Moreover, the performance of the Kagome HC-PCF implemented for NLOI is evaluated and validated by TPEF multispectral imaging of stained mouse tissue demonstrating its potential for biomedical applications. Fiber based alignment-free integration of an ultrafast laser excitation into a LSM poses the first step towards an endoscopic approach which might enable further wide-spread adoption and application of biomedical imaging with the fusion of a wealth of complementary imaging modalities. The described fiber delivery is highly versatile and fully compatible with existing nonlinear imaging techniques, including TPEF, SHG, and intrapulse coherent anti-Stokes Raman scattering (CARS) [28]. In particular, for CARS that is usually sensitive to nonlinear four-wave mixing induced by strong parasitic background coming from two pulses co-propagating [29], this technology can pose a big step towards real-world applications. Due to its large transmission window, it can also be used for other techniques, e.g., ultrahigh resolution optical coherence tomography. Simple fiber patch-cord for variable dynamic delivery [30] and the possibility for fusion splicing can help to facilitate taking this direction. Moreover, the fiber technology enables a combination of complementary techniques and implementation into endoscopes with novel double-clad collection concepts [31]. Hence, this delivery system opens novel perspectives, e.g., for intra-operative real-time histopathology where lasers can be kept outside the sterile environment since ultrashort light pulses can finally be delivered over long distances to the point of investigation.

Funding. Horizon 2020 Framework Programme (H2020) (H2020-PHC-2015, 667933); H2020 Marie Skłodowska-Curie Actions (MSCA) (721766).

Acknowledgment. The authors thank GLOPhotonics for support in fiber handling.

REFERENCES

1. W. R. Zipfel, R. M. Williams, and W. W. Webb, Nat. Biotechnol. **21**, 1369 (2003).
2. W. Denk, J. H. Strickler, and W. W. Webb, Science **248**, 73 (1990).
3. H. Choi and P. T. C. So, Sci. Rep. **4**, 6626 (2014).
4. P. Xi, Y. Andegeko, L. R. Weisel, V. V. Lozovoy, and M. Dantus, Opt. Commun. **281**, 1841 (2008).
5. I. Pastirk, J. M. D. Cruz, K. A. Walowicz, V. V. Lozovoy, and M. Dantus, Opt. Express **11**, 1695 (2003).
6. J. M. D. Cruz, I. Pastirk, M. Comstock, V. V. Lozovoy, and M. Dantus, Proc. Natl. Acad. Sci. USA **101**, 16996 (2004).
7. W. Liang, G. Hall, B. Messerschmidt, M.-J. Li, and X. Li, Light: Sci. Appl. **6**, e17082 (2017).
8. S. W. Clark, F. O. Ilday, and F. W. Wise, Opt. Lett. **26**, 1320 (2001).
9. A. M. Larson and A. T. Yeh, Opt. Express **16**, 14723 (2008).
10. W. R. Zipfel, R. M. Williams, R. Christie, A. Y. Nikitin, B. T. Hyman, and W. W. Webb, Proc. Natl. Acad. Sci. USA **100**, 7075 (2003).
11. F. Helmchen, D. W. Tank, and W. Denk, Appl. Opt. **41**, 2930 (2002).
12. G. P. Agrawal, *Nonlinear Fiber Optics*, 5th ed. (Elsevier/Academic, 2013).
13. R. Wolleschensky, T. Feurer, R. Sauerbrey, and U. Simon, Appl. Phys. B **67**, 87 (1998).
14. D. G. Ouzounov, K. D. Moll, M. A. Foster, W. R. Zipfel, W. W. Webb, and A. L. Gaeta, Opt. Lett. **27**, 1513 (2002).
15. C. Lefort, M. Kalashyan, G. Ducourthial, T. Mansuryan, R. P. O'Connor, and F. Louradour, J. Opt. Soc. Am. B **31**, 2317 (2014).
16. C. Lefort, T. Mansuryan, F. Louradour, and A. Barthelemy, Opt. Lett. **36**, 292 (2011).
17. F. G. Omenetto, A. J. Taylor, M. D. Moores, and D. H. Reitze, Opt. Lett. **26**, 938 (2001).
18. N. Cregan, N. Mangan, N. Knight, N. Birks, N. Russell, N. Roberts, and N. Allan, Science (New York) **285**, 1537 (1999).
19. D. G. Ouzounov, F. R. Ahmad, D. Müller, N. Venkataraman, M. T. Gallagher, M. G. Thomas, J. Silcox, K. W. Koch, and A. L. Gaeta, Science (New York) **301**, 1702 (2003).
20. F. Luan, J. Knight, P. Russell, S. Campbell, D. Xiao, D. Reid, B. Mangan, D. Williams, and P. Roberts, Opt. Express **12**, 835 (2004).
21. Y. Y. Wang, X. Peng, M. Alharbi, C. F. Dutin, T. D. Bradley, F. Gérôme, M. Mielke, T. Booth, and F. Benabid, Opt. Lett. **37**, 3111 (2012).
22. F. Benabid, J. C. Knight, G. Antonopoulos, and P. S. J. Russell, Science (New York) **298**, 399 (2002).
23. F. Couny, F. Benabid, P. J. Roberts, P. S. Light, and M. G. Raymer, Science (New York) **318**, 1118 (2007).
24. B. Debord, M. Alharbi, L. Vincetti, A. Husakou, C. Fourcade-Dutin, C. Hoenninger, E. Mottay, F. Gérôme, and F. Benabid, Opt. Express **22**, 10735 (2014).
25. J. S. Skibina, R. Iliew, J. Bethge, M. Bock, D. Fischer, V. I. Beloglasov, R. Wedell, and G. Steinmeyer, Nat. Photonics **2**, 679 (2008).
26. Y. Y. Wang, N. V. Wheeler, F. Couny, P. J. Roberts, and F. Benabid, Opt. Lett. **36**, 669 (2011).
27. B. Debord, M. Alharbi, T. Bradley, C. Fourcade-Dutin, Y. Y. Wang, L. Vincetti, F. Gérôme, and F. Benabid, Opt. Express **21**, 28597 (2013).
28. M. Andreana, T. Le, A. K. Hansen, A. J. Verhoef, O. B. Jensen, P. E. Andersen, P. Slezak, W. Drexler, A. Fernández, and A. Unterhuber, J. Biomed. Opt. **22**, 091517 (2017).
29. M. Balu, G. Liu, Z. Chen, B. J. Tromberg, and E. O. Potma, Opt. Express **18**, 2380 (2010).
30. B. Resan, R. Auchli, V. Villamaina, and R. Holtz, Opt. Express **25**, 24553 (2017).
31. A. Lombardini, V. Mytskaniuk, S. Sivankutty, E. R. Andresen, X. Chen, J. Wenger, M. Fabert, N. Joly, F. Louradour, A. Kudlinski, and H. Rigneault, Light: Sci. Appl. **7**, 10 (2018).